Computing the Flow Around a Submerged Body using Composite Grids

N. Anders Petersson & Johan F. Malmliden
Center for Computational Mathematics and Mechanics
Royal Institute of Technology, Sweden

(Submitted to the 6th International Workshop on Water Waves and Floating Bodies, April 1991)

1 Introduction

The subject of this paper is the use of composite overlapping grids together with finite difference methods to calculate free surface flows. In particular, the two dimensional steady potential flow around a submerged body moving in a liquid of finite constant depth at constant speed and distance below the free surface is considered. The motion is described in Cartesian coordinates which are fixed with respect to the body. The x-axis points opposite to the forward direction and the z-axis is directed vertically upwards. The total velocity potential is split into a free stream potential plus a perturbation potential, $\Phi = x + \phi$, and the boundary condition at the free surface is linearized around the free stream flow.

This problem can be solved by several existing techniques, like the boundary integral method described in [2] or the hybrid finite element method in [3]. The aim of the research described here is to take a first step towards an accurate method for the nonlinear potential problem, where the boundary integral method is known to depend on the addition of artificial dissipation at the free surface boundary. Another important reason was the prospect of incorporating effects by vorticity and viscosity.

2 The in and outflow boundary conditions

To solve the problem numerically, the infinite domain is truncated to $a \le x \le b$, where $b - a < \infty$. It is therefore necessary to impose in and outflow boundary conditions at $x = a$ and $x = b$ respectively. To achieve an accurate solution, it is of vital importance to minimize the influence of these artificial conditions. The method outlined below, and described in [4], allows for constructing boundary conditions that do not affect the solution of the present problem at all.

The solution is assumed to be bounded and satisfy the upstream condition at infinity. The boundary conditions are derived by making an eigenfunction expansion of the solution in the z-direction ahead of and behind the body,

$$\phi(x,z) = \sum_{k=0}^{\infty} \mathcal{R}^{(k)}(x)\mathcal{S}^{(k)}(z) \tag{1}$$

where

$$\mathcal{S}^{(0)}(z) = 1 \tag{2}$$
$$\mathcal{S}^{(1)}(z) = \cosh\sqrt{\lambda_1}(d+z) \tag{3}$$
$$\mathcal{S}^{(k)}(z) = \cos\sqrt{\mu_k}(d+z),\ k = 2,3,\dots \tag{4}$$

The corresponding eigenfunctions in the x-direction are given by

$$\mathcal{R}^{(0)}(x) = A_0 + B_0 x \tag{5}$$
$$\mathcal{R}^{(1)}(x) = A_1 e^{i\sqrt{\lambda_1}x} + B_1 e^{-i\sqrt{\lambda_1}x} \tag{6}$$
$$\mathcal{R}^{(k)}(x) = A_k e^{-\sqrt{\mu_k}x} + B_k e^{\sqrt{\mu_k}x},\ k = 2,3,\dots \tag{7}$$

To get a bounded solution, there must be no linearly growing modes ahead of or behind the body, ie. $B_0 = 0$. Moreover, there can only be exponentially decaying modes; $A_k = 0$ ahead of the body and $B_k = 0$ behind it for $k \ge 2$. The upstream condition implies that $A_1 = B_1 = 0$ ahead of the body. For these reasons, the linear mode must satisfy $d\mathcal{R}^{(0)}/dx = 0$ at $x = a$ and $x = b$. Furthermore, the exponentially decaying modes satisfy $d\mathcal{R}^{(k)}/dx = \sqrt{\mu_k}\mathcal{R}^{(k)}$ at

$x = a$ and $d\mathcal{R}^{(k)}/dx = -\sqrt{\mu_k}\mathcal{R}^{(k)}$ at $x = b$. Finally, the oscillatory mode must have $\mathcal{R}^{(1)} = 0$ and $d\mathcal{R}^{(1)}/dx = 0$ at $x = a$. These conditions on the Fourier side are transformed to conditions on ϕ by first noting that

$$\langle \mathcal{S}_z^{(p)}, \mathcal{S}_z^{(q)} \rangle_2 = 0, \; p \neq q, \tag{8}$$

where $\langle f, g \rangle_2$ is the $\mathcal{L}_2$ scalar product. The coefficients can then be found by

$$\mathcal{R}^{(k)}(x) = \frac{\langle \phi_z(x, \cdot), \mathcal{S}_z^{(k)} \rangle_2}{\|\mathcal{S}_z^{(k)}\|_2^2}, \; k = 1, 2, \ldots \tag{9}$$

and

$$\mathcal{R}^{(0)}(x) = \phi(x, -d) - \sum_{k=1}^{\infty} \frac{\langle \phi_z(x, \cdot), \mathcal{S}_z^{(k)} \rangle_2}{\|\mathcal{S}_z^{(k)}\|_2^2} \mathcal{S}^{(k)}(-d) \tag{10}$$

This approach is also possible when the problem is discretized by finite differences on a Cartesian grid. Here the boundary conditions are matrix relations between the value and the normal divided difference of the solution at the in and outflow boundaries. Let the grid sizes in the x and z-directions be $h_x = (b - a)/(N - 1)$ and $h_z = d/(M - 1)$ and let the grid points in the Cartesian grid be $x_j = a + (j - 1)h_x$ and $z_k = -d + (k - 1)h_z$. The boundary conditions can be written as

$$A\mathbf{u}_1 + B\frac{1}{2h_x}(\mathbf{u}_2 - \mathbf{u}_0) = 0 \tag{11}$$

$$C\mathbf{u}_N + D\frac{1}{2h_x}(\mathbf{u}_{N+1} - \mathbf{u}_{N-1}) = 0 \tag{12}$$

where A and B are $(M + 1) \times M$ matrices. C and D are $(M - 1) \times M$ matrices and the vector $\mathbf{u}$ is given by

$$\mathbf{u}_j = (\phi(x_j, z_1), \phi(x_j, z_2), \ldots, \phi(x_j, z_M))^T \tag{13}$$

The matrices A, B, C and D are derived from the discrete counterpart of the eigenfunction expansion and scalar product; they are not merely discretized versions of the continuous boundary conditions.

3 The composite grid

To be able to handle bodies of general shape, it is convenient to discretize the domain close to the body with one or several body fitted curvilinear grids. This makes the discretization of the Neumann boundary condition on the body accurate and straightforward. The need for both a Cartesian and a curvilinear grid is satisfied by utilizing a composite grid, Fig. 1. The composite grid method is a general tool for solving PDE's on complex domains, cf. [1]. The basic idea is to divide the complex domain into simple overlapping subdomains, the union of which completely covers the region of interest. Each subdomain is covered by a component grid. This set of component grids taken together is called a composite grid. The component grids overlap each other with no requirement that they exactly match up at their edges. The main advantage compared to covering the whole domain with one single grid is that each component grid can be chosen to have a smooth transformation to the unit square; in particular be made without singularities. To solve a PDE on a composite grid, it is first transformed to the unit square of each component grid. The transformed PDE is then approximated by finite differences. The component grid problems are coupled to each other by interpolation at the interior boundaries where the subdomains overlap.

In the present method, a second order accurate finite difference method is used on the component grids. To get second order accuracy for the total solution it is necessary to use third order accurate interpolation (biquadratic).

The grid generation program CMPGRD, cf. [1], was employed to construct the composite grids. This program supplies as output all the information needed to form the difference equations and the interpolation relations. Furthermore, CMPGRD is capable of constructing 3–D composite grids, so the present method can be extended to 3–D problems.

The resulting sparse linear system of equations was solved by LU-decomposition followed by iterative improvement until the norm of the residual did not decrease further. From a computational point of view, the main difficulty of extending the present method to 3–D lies in the solution of the sparse linear system. An fast iterative solver based on domain decomposition is under current development.

a_1	b_1	a_2	b_2	$\|\phi_1 - \phi_2\|_\infty$	$\|\phi_1\|_\infty$
-5.4	5.4	-2.7	2.7	9.47×10^{-6}	5.31

Table 1: Extension of the solution by the eigenvector expansion.

4 Numerical examples

The following experiment was done to investigate the quality of the boundary conditions at $x = a$ and $x = b$. Two solutions ϕ_1 and ϕ_2 were computed around a test body. The computational domains in the x-direction were $a_1 < x < b_1$ and $a_2 < x < b_2$ respectively, where $a_1 \ll a_2$ and $b_2 \ll b_1$. After the solution in $a_2 < x < b_2$ had been calculated, it was extended to $a_1 < x < b_1$ by the discrete counterpart of the eigenvector expansion. To make it easier to compare the two solutions, a constant was added to each of them such that $\phi_j(a_1, 0) = 0$. A circular cylinder of radius R was used as test body and the non-dimensional depth was $d = 5R = 7.8125$. The distance between the surface and the center of the cylinder was $2R$. The shorter of the grids is shown in Fig. 1. The longer grid was identical to the shorter grid in $a_2 \leq x \leq b_2$, but the Cartesian component grid was extended to $a_1 \leq x < a_2$ and $b_2 < x \leq b_1$ by increasing the number of grid points and keeping the grid size unchanged. The difference, $\phi_1 - \phi_2$, measured in maximum norm over $a_1 < x < b_1$ is given in Table 1. The conclusion of the experiment is that the difference is negligible. Obviously, there is a considerable gain in decreasing $b - a$; the number of equations decreases and the solution close to the body becomes less sensitive to roundoff errors, since the eigenvalue of smallest magnitude of the discrete operator behaves like $(b - a)^{-2}$, cf. [4].

To exemplify the use of the present method, the flow about ellipses and rounded rectangles was studied as function of the length of the bodies at a fixed Froude number. In particular, the lift and drag coefficients were calculated. In all computations, the non-dimensional depth was fixed to $d = 5$ which yielded a Froude number $F_d = 1/\sqrt{5} \approx 0.447$. The ellipses had the horizontal semiaxis submerged $0.5d$ below the surface and the length of the vertical semi axis was $0.1d$. The streamlines around the ellipse of nondimensional length 3.0 are presented in Fig. 2. The thickness of the rounded rectangle was set to $0.2d$, the radius of the rounded ends to $0.1d$ and the upper horizontal boundary was submerged $0.4d$ below the surface. The results are given in Fig. 3. The lift and drag coefficient were based on half the total length of the bodies. The minima in C_D occur for different lengths for the two geometries which implies that the more slenderly shaped ellipse does not always generate less drag than the rounded rectangle.

5 Conclusions

In this paper, it has been shown that composite grids together with finite difference methods can be used to calculate the linearized potential flow around a submerged body. To treat the nonlinear case with a wavy surface, the plan is to add a third component grid close to the surface. The above described inflow boundary condition can be used for the nonlinear problem if that boundary is located sufficiently far ahead of the body. Behind the body, where the solution is known to oscillate, it is not possible to use the technique from linear theory to construct the outflow boundary condition. An alternative approach is under current development.

References

[1] G. CHESSHIRE AND W. D. HENSHAW, *J. Comput. Phys.* **90**, 1 (1990)

[2] C. W. DAWSON, in *Proceedings of the Second International Conference on Numerical Ship Hydrodynamics, Berkely, 1977*, p. 30.

[3] C. C. MEI AND H. S. CHEN, *Int. J. Num. Meth. Eng.* **10**, 1153 (1976).

[4] N. A. PETERSSON, "Numerical Methods to Calculate the Linear and Nonlinear 2–D Flow Around an Underwater Obstacle", Thesis, Dept. of Numerical Analysis and Computing Science, Royal Institute of Technology, Internal Report TRITA–NA–9001, 1990 (unpublished).

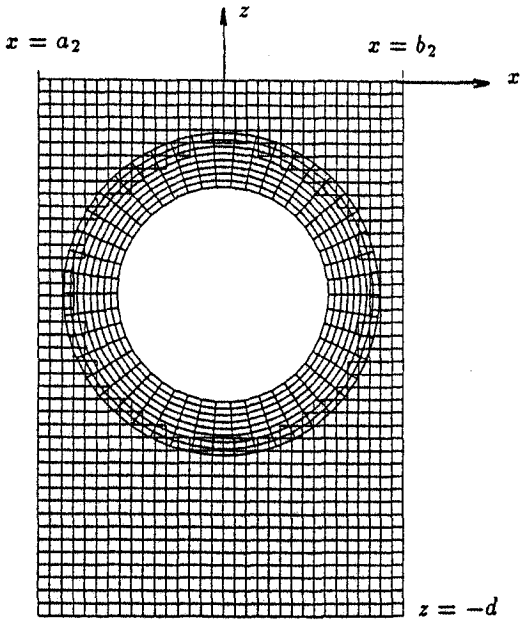

Figure 1: The shorter composite grid in the test of the in and outflow boundary conditions.

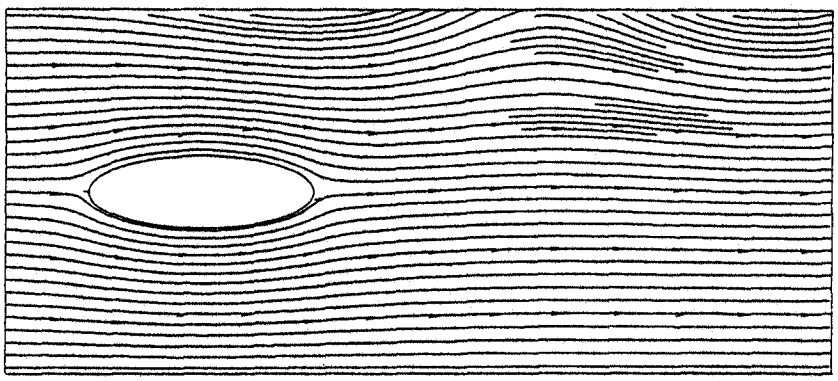

Figure 2: Streamlines around the ellipse of length 3.0.

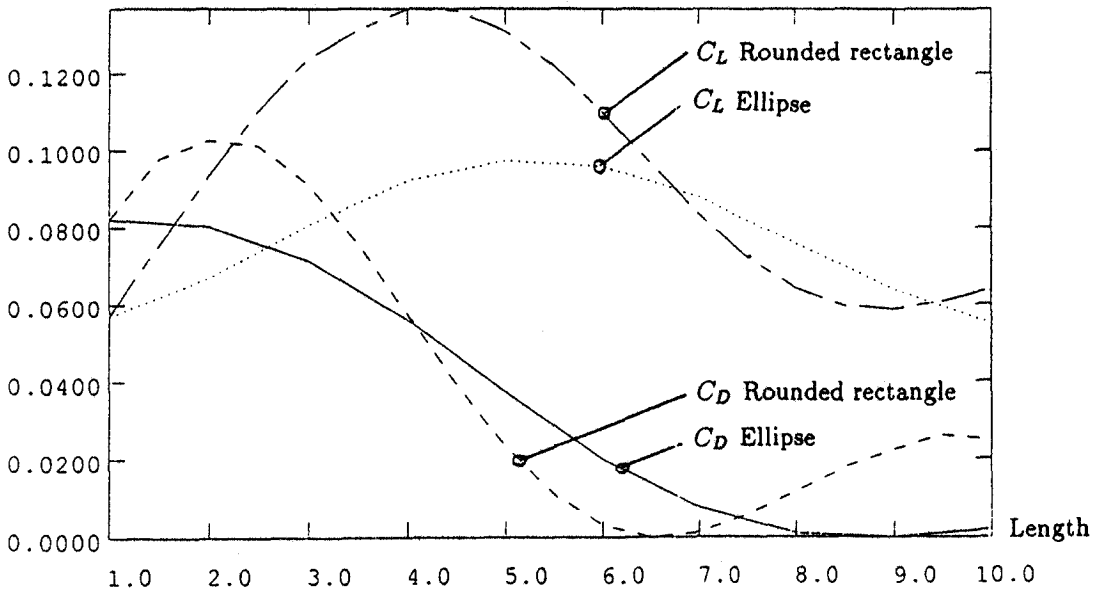

Figure 3: The lift and drag coefficients as function of the length of the ellipse and the rounded rectangle.

Tuck: Further to Fig. 2., I believe that it is possible for some of the streamlines above $z = 0$ to be non-continuous *i.e.*, to rise to infinity. This is a consequence of linearization, which is inconsistent with full streamline plotting. (This effect might not occur at the submergence shown since there is a critical extent to the nonlinearity, see my 1965 JFM paper on submerged circular cylinders.)

Peterssen & Malmliden: For bodies with smaller submergence then the one in Fig. 2, we have experienced cases where the streamlines turn forward behind the body, close to the surface. We agree with Prof. Tuck that this indicates that the solution of the linearized problem describes reality very poorly. However, we think that it is necessary to first define the problem in the region above $z = 0$ before discussing the behavior of streamlines in that domain.